Deutscher Luft- und Raumfahrtkongress 2008
DocumentID: 81298

Comparison of slot injector and lobed injector and their application to supersonic combustion

J. Chun, T. Scheuermann, J. von Wolfersdorf, and B. Weigand
Universität Stuttgart, Institut für Thermodynamik der Luft- und Raumfahrt (ITLR),
Pfaffenwaldring 31, 70569 Stuttgart, Germany

Abstract

Mixing and combustion performances of a slot injector and a lobed injector in a scramjet combustor model were experimentally investigated using planar laser Mie scattering technique and a high speed camera, respectively. A slot injector has a slot along the spanwise direction, whereas the lobed injector has four lobed structures enlarging the contact area between air and fuel thereby enhancing mixing performance. Both injectors have internally small convergent-divergent nozzles, through which the fuel is accelerated to supersonic speed. They were tested for several injection pressures and combustor inlet pressures using helium and air as injectants. The mixing layer of the slot injector increased linearly. Even though there were some variations of the growth rate of the mixing layer according to their injection conditions, the mixing regions were, however, confined in the core region of the combustor; the fuel from the slot injector could not diffuse well into the co-flow. On the other hand, the macroscopic streamwise vortex structures generated by the lobed injector stirred the mixing region very well and the injectant mixed with the main flow in a short distance after injection. In the followed combustion tests, the lobed injector showed higher performance than the slot injector, but not increased such a strong performance as in the mixing experiment. The photos using the high speed camera revealed that the ignition occurred far downstream from the injection and the flame traveled upstream. This mechanism diminished the enhanced mixing performance of the lobed injector in the combustion test.

1 Introduction

One of the important and challenging applications of the compressible mixing and combustion is high speed propulsion system. Even though it is obvious that the scramjet engine is a strong candidate for future high speed propulsion systems, the scramjet engine has still technical problems to overcome. One of them is the short residence time of fuel in the combustor. Under normal operation conditions, the residence time is only on the millisecond scale. In these short time, the fuel should be injected, mixed, ignited, reacted and exhausted. Therefore, the stable mixing and combustion are of critical importance in the development of the scramjet propulsion system.

Several injection mechanisms, which play key roles in the mixing and combustion in the scramjet engine, have been paid attention to for several decades. They can be, in general, divided into two categories; wall injection and parallel strut injection. As Chun et al. [1] pointed out, the parallel strut injection has several advantages over the wall injection such as the usage of the fuel momentum, the suppress of boundary layer separation, and the low aerodynamic loss. This is especially true if we are interested in civil applications of scramjet engines, where normally the combustion chamber has larger dimensions than for military applications.

In the present study, hence, the mixing performances of the two different central strut injectors were tested; a flat injector and a lobed injector. The lobed injector has lobed structures at the trailing edge of the injector, which generate streamwise vortices. In addition, combustion tests using the two injectors were also conducted to investigate how the mixing performances of the two injectors influence the combustion performances. These tests were conducted using the supersonic test facilities of ITLR, Universität Stuttgart, Germany. More details about the test facilities is given in the following section.

2 Experimental Investigation

2.1 ITLR supersonic test facilities

The ITLR supersonic test facility composed of a screw compressor, a three-staged electric heater, and the test section. The screw compressor was capable of continuously delivering air at a maximum of 10 bar with a flow rate of 1.45 kg/s. Benefits of the screw compressor were not only that it enabled continuous experiments, but it presented also the possibility to change the total pressure easily, even during an experiment. The air could be heated up to maximum 1500 K using the electric heater of 1MW electric power and was introduced via a 2.1 Mach number Laval nozzle into the scramjet model combustor. This test facility simulated a flight Mach number of approximately 5 to 6. The air supplied to the model combustor was free of vitiation.

2.2 Model Combustor

The model combustor used in the present study is illustrated by Figure 1. It had a 226 mm long isolator, a 372 mm long fixed diverging part (FD) , and a 720 mm long variable diverging part (VD). The isolator in a scramjet is required to have two functions. The first one is to provide "ignitable" condition in the combustor. The air captured at the inlet of the engine is compressed by a series of shock waves in the isolator, thereby it is heated up to the ignition temperature of the fuel in the combustor. The second function is to prevent the flame to travel upstream to the inlet of the scramjet engine. Otherwise, the amount of air captured at the inlet decreases drastically during flight and the engine can not work properly. The following diverging parts were the sections where the combustion took place. The divergence of the combustor was designed to avoid thermal choking due to heat release from the combustion. The FD had a fixed opening angle of 1°, whereas the VD which composed of two parts, namely VD1 and VD2, could adjust its opening angle up to 3°. The lengths of the VD1 and VD2 were 372 mm and 348 mm, respectively.

2.3 Instrumentations

Wall static pressures on the top of the model combustor were measured by a pressure scanner which had 64 pressure transducers. Their uncertainties were less than ±7 kPa. The measured wall pressures were averaged over half a second. Note that some of the pressure tabs formed a module block which could be exchanged with the quartz windows enabling a laser sheet to access to the flow.

The total pressure and the total temperature of the main air stream were measured at the exit of the second heater. The total pressure was measured using pressure transducers having a large measurement range (uncertainty ±10 kPa). The total temperature was determined by averaging three K-type thermocouples whose uncertainties were ±1.0 %.

The mass flow rate of the air stream was measured with a vortex flow-meter in combination with temperature and pressure instruments (combined uncertainty less than: ±9.0 %). A magnetic valve controlled the fuel flow amount and a mass flow-meter measured the mass flow rate of the fuel whose uncertainty was maximum ±5.0%.

2.4 Injectors

The flat injector illustrated in Figure 2 provided a basic data set for the mixing process since it had a planar shape enabling to assume a two dimensional mixing process. The length and the width of the injector were 80 mm and 40 mm, respectively. It was designed as a double-wedge and has a maximum thickness of 6 mm. The trailing edge thickness and the injection slot height were 2 mm and 0.7 mm, respectively.

It is well known that the growth rate of the mixing layer is drastically reduced by high convective Mach number. To overcome this compressibility effect, lobed injectors has been suggested by several researchers and theoretical [2], numerical [3], and experimental studies [4], [5] have been conducted. The lobed injector used in the present study is shown in Figure 3. It had 4 lobed structures and the width of each structure was 10.5 mm. The length and the width of the injector were 86 mm and 40 mm, respectively. Note that the lobed injector was longer than the flat injector. The trailing edge thickness of the injector was 1.3 mm. The injection slot height and the lip thickness at the trailing edge are 0.7 mm and 0.3 mm, respectively.

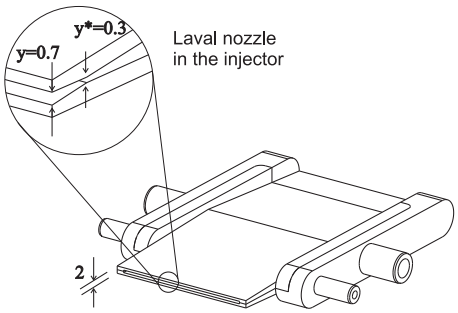

Figure 2: Flat injector

It is noteworthy that both injectors had internally small Laval nozzles along the injectant flow path in vicinity of the trailing edge, as shown in the details of Figure 2 and Figure 3. The area ratios of the exit and the throat of these Laval nozzles were 2.3 for both injectors. The isentropic Mach numbers of the injection with air and helium were 2.4 and 2.6, respectively.

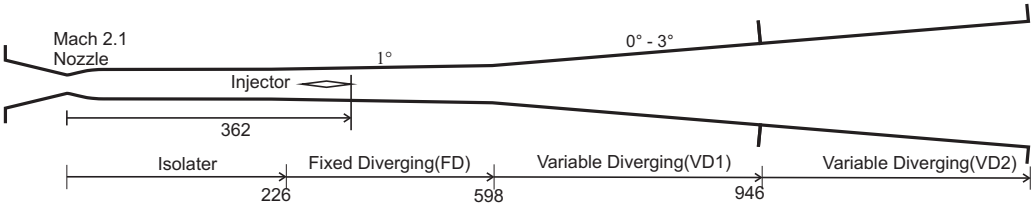

Figure 1: Schematic of the model combustor

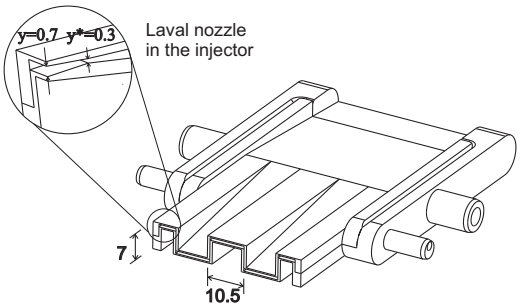

Figure 3: Lobed injector

3 Measurement Techniques

The mixing behavior was visualized using the Planar Laser Mie Scattering (PLMS) method. A frequency-doubled Nd:YAG laser of 532 nm (New Wave, Gemini PIV) with a 30 mJ/pulse was used with a 10 Hz repetition rate. The laser beam was formed to a sheet whose typical width and thickness were about 10 cm and 0.3 mm, respectively. The laser sheet was introduced into the test section through the slot windows on the bottom of the test section, as illustrated in Figure 4a depicting a top view of the test section. An intensified-CCD camera (DaVis, FlowMaster) whose maximum resolution was 1280 x 1024 was used to collect the scattered light. Using this configuration, streamwise PLMS images in the test section were taken.

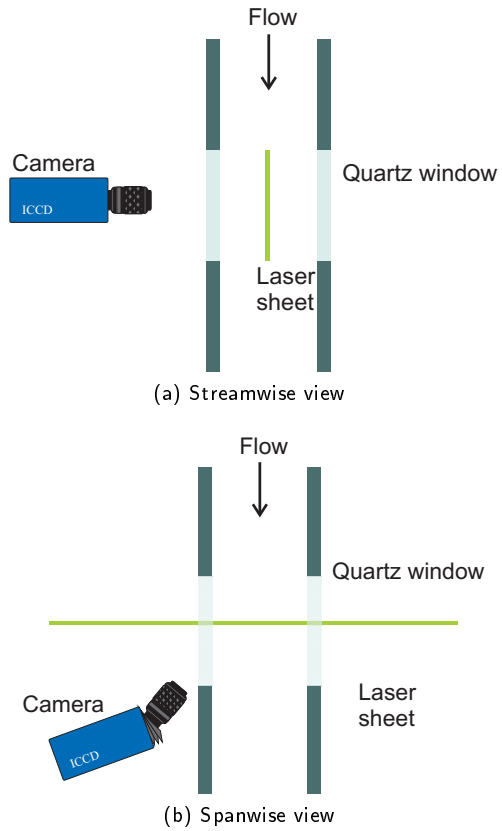

Figure 4: Top view of the test section and the optics configuration

The lobed injector generates streamwise vortices which can not be captured by the above configuration. Hence, in order to capture the spanwise images in the combustor, another additional optical configuration was used. Look at Figure 4b. The laser sheet was introduced into the test section through a side window. The camera was located beside the test section and collected the scattering light obliquely. The Scheimpflug principle was applied to correct the problem arising from the oblique viewing angle under this configuration.

In the present study, 1 μm TiO_2 was used as the seeding particle which was laden to the injectant using a seeding generator. The seeding generator was a kind of fluidized-bed particle dispenser where pressurized flow transported the particles into the stream and the particle-laden flow entered the injector. Because the particles in the container tend to agglomerate, a 2 mm diameter sonic orifice was used at the exit of the generator to generate strong shear stresses thereby to disperse effectively the agglomerated particles. This type of seeding generator was successfully applied to a PIV (particle image velocimetry) measurement in a combustor by Willert and Jarius [6].

4 Results and Discussions

4.1 Flow-field without injection

Because the injector was placed in the center of the combustor, its leading edge precipitated shock waves around the injector. As it can be seen in the pressure distribution in the combustor (Figure 5), high pressure peaks appeared in vicinity of the injector.

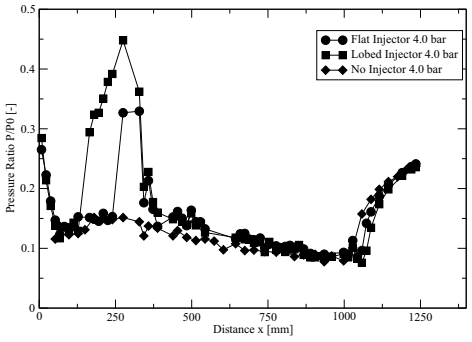

Figure 5: Pressure distributions with and without the injector

It is interesting that the static pressure distributions of the flat and the lobed injector showed significant differences in vicinity of the injector. The onset point of the pressure rise for the lobed injector is located more upstream than that for the flat injector. In addition, the peak pressure of the lobed injector is much higher than that of the flat injector.

Considering the boundary layer separation limit suggested by Heiser and Pratt [7], the boundary layer with

the lobed injector was supposed to be separated and the separated boundary layer to invoke a series of shock waves. This series of shock waves is known as a pseudo-shock wave which plays an important role in a supersonic application. The separation bubble of the pseudo-shock wave moved the onset point of the pressure rise toward upstream. The schlieren image taken in vicinity of the lobed injector (Figure 6) shows the pseudo-shock wave very clearly.

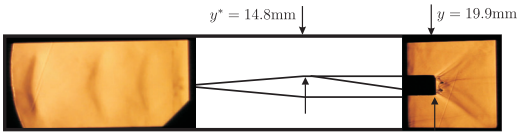

Figure 6: Schlieren image around the lobed injector

On contrast, the flow-field with the flat injector didn't seem to be accompanied by the boundary layer separation, thereby no pseudo-shock wave appeared because the pressure rise in vicinity of the injector was low. Schlieren images (Figure 7) showed also that there is no pseudo-shock wave.

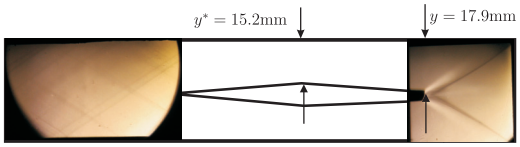

Figure 7: Schlieren image around the flat injector

It should be pointed out that oblique shock waves at the trailing edges of the two injectors showed that the flows in vicinity of the trailing edge were supersonic. The flow downstream of a pseudo-shock wave is normally subsonic as stated by Matsuo et al. [8]. However, the throat of the flow path between the model combustor wall and the height of the injector played a kind of Laval nozzle and the subsonic flow downstream of the pseudo-shock wave accelerated through this throat and became again supersonic in vicinity of the injector trailing edge.

From the area ratio between the choked area and the area at the trailing edge, we could get the Mach numbers downstream of the pair of the oblique shock waves. They were 1.4 and 1.7 for the flat injector and the lobed injector, respectively. And they agreed very well with the Mach numbers from the schlieren images in Figure 6 - 7.

The pressure rise at the exit of the model combustor represents the over-expansion of the supersonic flow. The pressure distributions of both injectors show little difference in this region. This means that the effects of the injector type do not influence the far-downstream flow field.

4.2 Mixing performance of the flat injector

In the next two sections, the mixing performance of the flat and the lobed injector using the PLMS technique will be investigated.

Helium and air were used as injectants in the investigation of the mixing performance of the flat injector. The injection pressure and the total pressure of the main air stream were varied ,which are summarized in Table 1. Note that p_0 and p_{in} in Table 1 denote the total pressures of the main air stream and the injectant in the injector, respectively.

Table 1: Injection conditions for the flat injector

Case Nr	p_0 [bar]	p [bar]	Gas	p_{in} [bar]	p/p_{in} [-]
P1	3.0	0.6	He	1.4	0.42
P2	3.0	0.6	He	1.9	0.32
P3	5.0	1.0	He	2.1	0.49
P4	7.0	1.4	He	2.0	0.69
P5	3.0	0.6	Air	1.2	0.51
P6	5.0	1.0	Air	1.9	0.52
P7	7.0	1.4	Air	2.0	0.69

Figure 8 illustrates typical instantaneous and averaged PLMS images of the flat injector, which show well the large-scale vortical structure of the mixing region. From the averaged PLMS image, it can be seen the mixing region grew slowly with the distance. But, it should be noticed that the mixing region was confined in the middle of the combustor, which means that the injectant did not diffuse into the co-flow effectively.

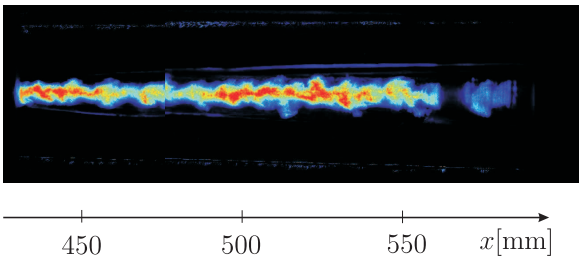

(a) Instantaneous PLMS image

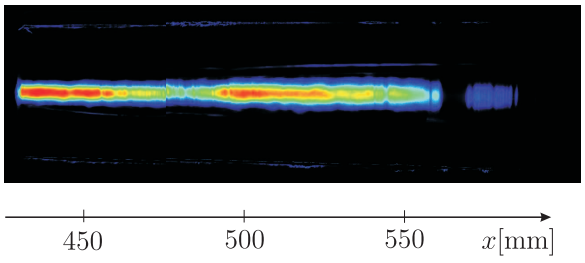

(b) Averaged PLMS image

Figure 8: PLMS images of flat injector

Figure 9 shows the half width of the visible mixing region, δ, of each case. The figure clearly indicates the growth of δ. What is interesting with δ is that it did not change very much even though the variation of the test conditions (P1 to P7) were relatively large.

Normally convective Mach number, $\mathrm{M_c}$, is used to describe the reduced compressible mixing layer growth

rate [9]. The convective Mach number in the present study was about 0.2 to 0.5 at the near-field of the injector. However, since the injection hole's width is very small (0.6 mm), as Gelinger and Brüggemann [10] pointed out, the velocity differences between the main air stream and the injectant became negligible in a short distance. Therefore, the convective Mach numbers at the measurement points of about 100 mm downstream from the injection point were very low and the compressibility effects were small.

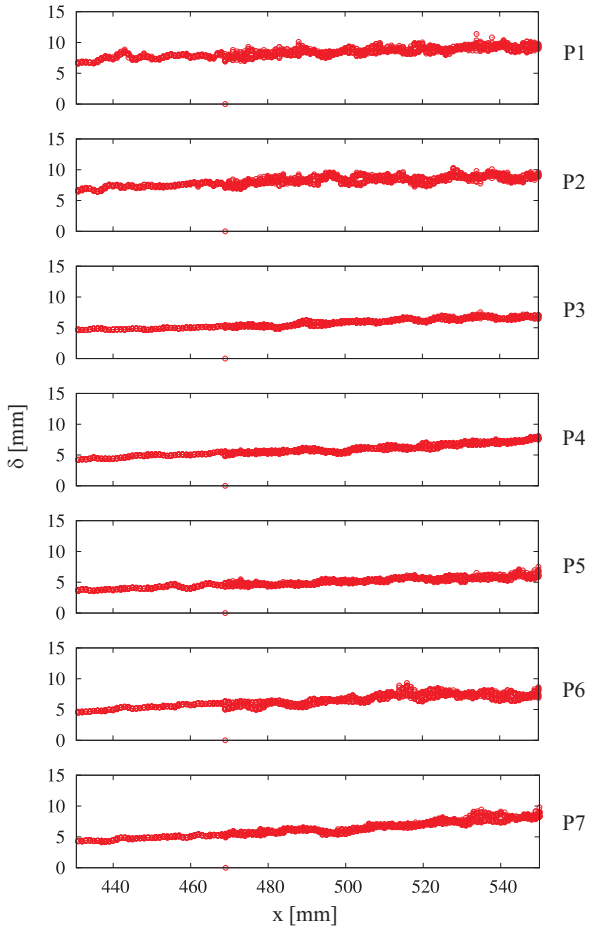

Figure 9: The mixing width, δ, for the flat Injector, where x is the distance from the throat of the Laval nozzle

Figure 10 shows the mixing layer growth rate, $\delta^{'}$, as a function of the momentum flux ratio of the injectant and the co-flow air stream. Note that $\delta^{'} = d\delta/dx$ was obtained using a linear fit over all data points in Figure 9. As it can be seen from the figure, the growth rates increased with higher momentum flux ratios. Hence, the higher momentum flux of the injectant was, the wider the mixing region was. Recalling that the velocity differences between the jet and the co-flow air stream at the measurement points were almost zero, the growth rate, $\delta^{'}$, was not affected by the far-downstream conditions. Rather it was strongly influenced by the initial injection conditions.

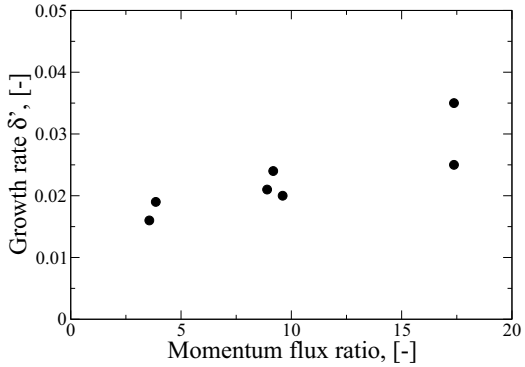

Figure 10: Mixing layer growth rate as a function of momentum flux ratio of the injectant and the co-flow air stream

4.3 Mixing performance of the lobed injector

The lobed injector was tested under similar injection conditions as the flat injector. Table 2 summarizes the injection conditions for the lobed injector. The total pressure in the main air stream was set to have the same values as for the flat injector's cases.

Table 2: Injection conditions for the lobed injector

Case Nr.	p_0 [bar]	p [bar]	Gas	p_{in} [bar]	p/p_{in} [-]
R1	3.0	0.6	He	1.4	0.4
R2	3.0	0.6	He	2.1	0.3
R3	5.0	1.0	He	2.0	0.5
R4	5.0	1.0	He	2.3	0.4
R5	7.0	1.4	He	2.0	0.7

The lobed injector showed different performance. Figure 11 shows the spanwise averaged PLMS images for the lobed injector. The images represent that the streamwise vortices generated by the injector's lobed structure enlarged the mixing region and the contact area. The mushroom pattern of the vortices at the centerline of the combustor at x = 462 mm started to be washed out at x=497 mm and were disappeared at x=527 mm. Simultaneously the height of the injectant grew and the mixing region became wider as the injectant flowed downstream. As can be seen in the figure, the injectant filled almost the channel at x=527 mm.

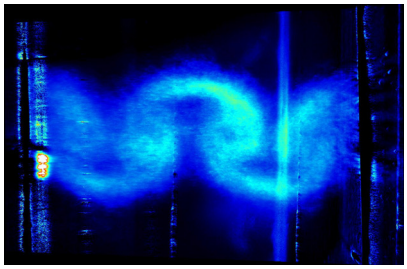

(a) x = 462 mm

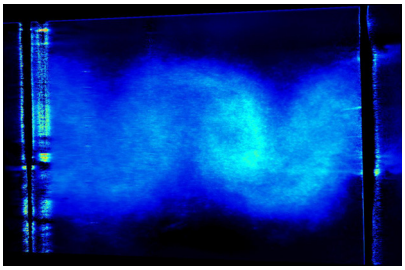

(b) x = 497 mm

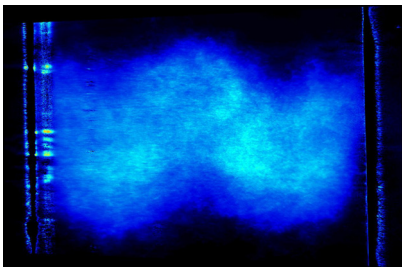

(c) x = 527 mm

Figure 11: Averaged PLMS images of the lobed injector

Side views for the lobed injector are shown in Figure 12. Comparing the mixing region for the flat injector, the images show obviously that the width of the mixing region was much larger.

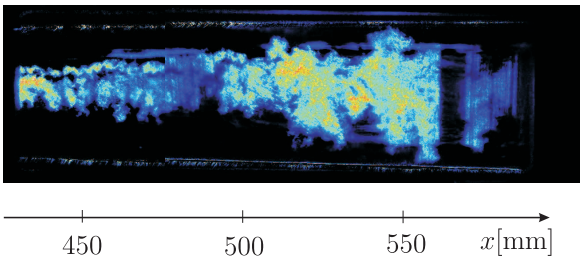

(a) Instantaneous PLMS image

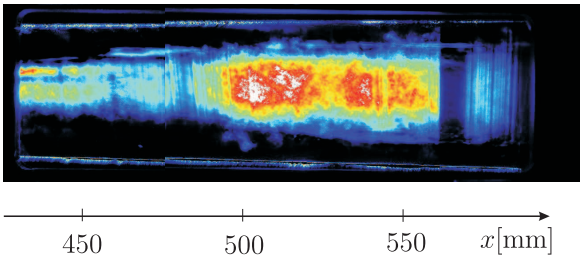

(b) Averaged PLMS image

Figure 12: PLMS images for the lobed injector

Figure 13 shows a mixing performance comparison between the flat injector and the lobed injector. For this comparison, the case P4 for the flat injector and the case R5 for the lobed injector were chosen. The two cases had the same injection conditions and differed only in the injector type. The mixing performance was defined as the area the injectants occupied in the model combustor divided by the cross-sectional area of the model combustor at this point. Assuming the mixing region for the flat injector was two-dimensional, its mixing performance for the case P4 was then simply the ratio of the mixing width, δ, and the height of the combustor.

The mixing region for the lobed injector was, however, three-dimensional. Hence, the mixing performance for the case R5 could be only obtained from the spanwise PLMS images like Figure 11, where the number of the pixels higher than the threshold value were divided by the number of the pixels of whole cross-sectional area of the combustor. As Figure 13 shows, the injectant from the lobed injector occupied wider areas than that of the flat injector.

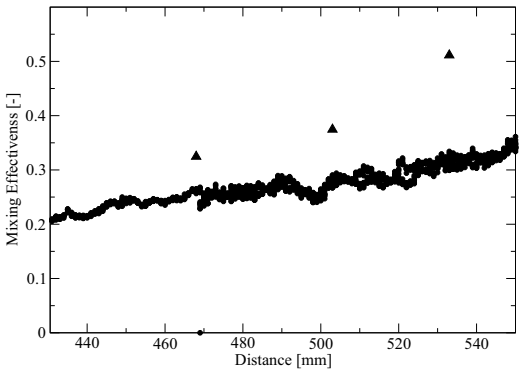

Figure 13: Comparison of mixing effectiveness of flat and lobed injector (Circle : case P4 , Triangle : case R5)

It is interesting to look at the normalized RMS (Root Mean Square) images of the PLMS for both injectors, as shown in Figure 14. The bright color in the figure indicates high normalized RMS whereas the dark color indicates low values. As it can be seen from the figure, the mixing region of the lobed injector had a larger region with bright color than that of the flat injector. Since the high value of the normalized RMS indicates high fluctuation of the seeded fluid flow, the mixing region with high RMS values had higher fluctuations thereby it was easy for the injectant to mix with the co-flow.

The lobed injector shows enhanced mixing performance not only in the enlarged contact area between the injectant and the co-flow, but also in the mixing quality which may be evaluated from the normalized RMS values of the seeded fluid.

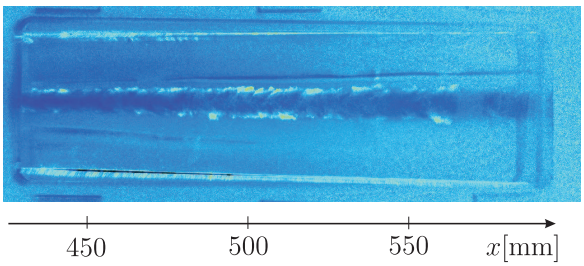

(a) flat injector

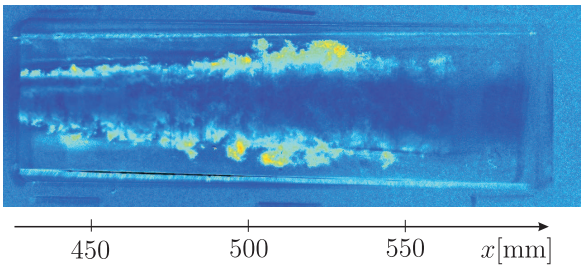

(b) lobed injector

Figure 14: Normalized RMS images of the two injectors

4.4 Application to Combustion

Until now we have discussed the enhanced mixing performance of the lobed injector, compared with the flat injector. Now we will investigate whether the combustion efficiency of the lobed injector may be also as much enhanced as its mixing performance, compared with the flat injector.

The total temperature of the main air stream in the combustor was increased to 1400 K. The total pressure was held at 4.0 bar. Once the total temperature reached the target value, then the fuel, hydrogen, was injected through each injector and the fuel amount was raised stepwise.

During the test, two different combustion modes were observed with respect to equivalence ratio, ϕ. Note that ϕ is defined as the ratio of the fuel-to-air ratio to the stoichiometric fuel-to-air ratio. The flames were located far downstream with a small equivalence ratio and moved slowly upstream as the equivalence ratio increased. At a certain equivalence ratio, the flame jumped from far downstream to the end of the injector and attached to the injector with a bright illumination and different wall pressure distributions. The first combustion mode is called weak combustion and the second strong combustion, respectively. Figure 15 shows photographs of each combustion mode. More details about the two combustion modes can be found elsewhere [1], [11].

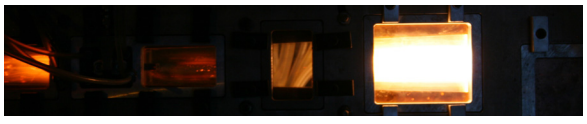

(a) weak combustion

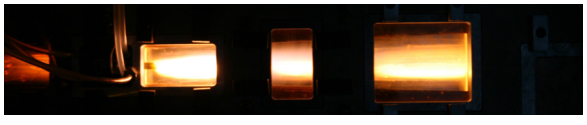

(b) strong combustion

Figure 15: Photos of the two combustion modes

The wall pressure distribution in the combustor along the axial distance from the flat injector is shown in Figure 16a. Remember that the pressure rise in vicinity of the combustor exit with no-injection ($\phi = 0$) was attributed to the over-expansion of the flow in the combustor. With a low equivalence ratio, $\phi = 0.17$, the onset point of the pressure rise due to combustion moved slowly upstream; weak combustion. But, for the strong combustion ($\phi = 0.28$), the pressure rise began directly downstream of the injector. These were consistent with the photos in Figure 15.

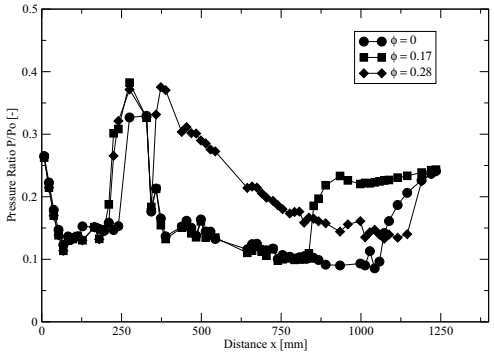

(a) The flat injector

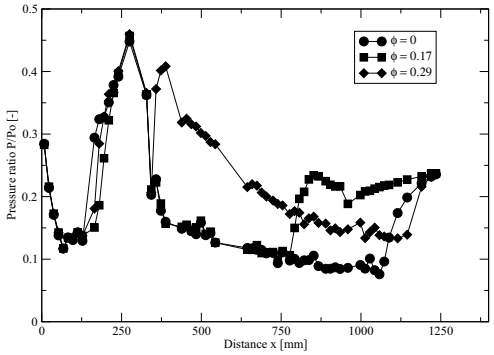

(b) The lobed injector

Figure 16: Static pressure distributions of the weak and the strong combustion (Po : 4 bar, To : 1400 K)

The total temperatures of these tests were 1400 K and the auto-ignition temperature of the hydrogen is about 850 K at this test conditions [12]. The static temperature in the combustor around the ignition point might be lower than the ignition temperature of the hydrogen. Chun et al. [1] reported that the ignition of the weak combustion was achieved by the pseudo-shock wave in vicinity of the exit of the combustor. They used a shorter combustor and it was hard to distinguish the two onset points of the pseudo-shock wave and the pressure rise due to combustion. This reveals that the high temperature region precipitated by the pseudo-shock waves attributes to the ignition of the fuel.

The lobed injector showed very similar pressure dis-

tributions as for the case of the flat injector, as shown in Fig 16b. It showed also the two combustion modes. Its onset point and its peak point of pressure rise in the weak combustion moved a little bit more upstream and was higher than that of the flat injector, respectively. However, the enhancement of the combustion performance of the lobed injector was not as much as the mixing performance compared with the flat injector. This observation was also valid for the strong combustion.

One of the reasons for such a little difference between the flat injector and the lobed injector was the ignition mechanism by the pseudo-shock wave. Another reason was the transition mechanism of the two combustion modes, which will be more detail discussed in the following section.

The combustion mode transition mechanism is a very fast phenomena. In order to capture the transition, therefore, a high speed camera (Photron, VKI) was used. Figure 17 shows a series of the photos of the flame traveling upstream during the combustion mode transition. Even though it is not shown in the figure, the flame showed some level of fluctuations prior to the begin of the transition. Once triggered, then the flame moved upstream with a speed between 120 m/s and 150 m/s with respect to the laboratory frame (See (a) - (d)). The traveling flame past even over the trailing edge of the injector, ((f) - (g)) and it came quickly back to the trailing edge (Figure 17h) and established a stabilized flame at the trailing edge (Figure 17i).

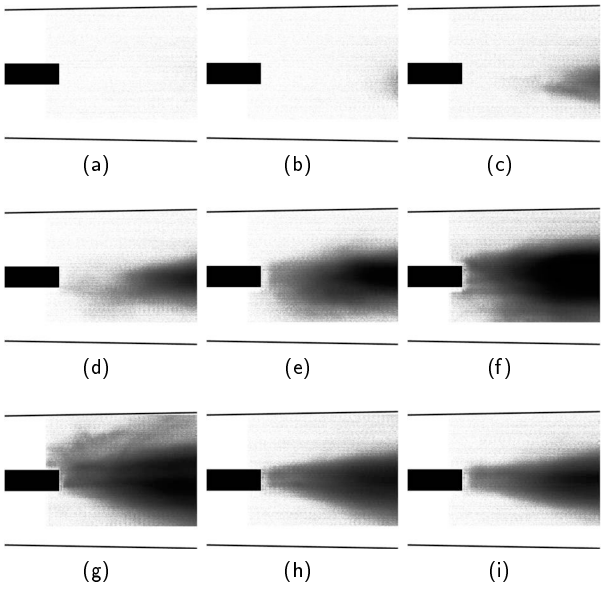

Figure 17: Images taken during the combustion mode transition (black box indicates the trailing edge of the injector. The time step between each image is 1 ms. Images from [11])

As previously pointed out, the upstream traveling velocity was between 120 m/s and 150 m/s with respect to the laboratory frame. If we sit on moving air molecule and observe the upstream traveling flame in the relative frame, then it moves upstream with a supersonic velocity. Sunami et al. [13] observed also a similar combustion mode transition and showed the transition accompanies a kind of Chapman-Jouget detonation wave. The shock waves accompanying the detonation wave might change drastically the mixing and combustion pattern of both injectors. Hence the enhanced performance of the lobed injector in the mixing test could not be anymore observed in the combustion test.

5 Conclusions

Using the PLMS technique, the mixing behaviors of a flat injector and a lobed injector were experimentally investigated and the following major outcomes were obtained.

- The injectant from the flat injector remains mostly in the mid of the combustor and it does not provide effective mixing in the scramjet combustor.
- The lobed injector generates streamwise vortices, which enlarge the contact area between the air and the fuel. So, it enhances the mixing in the combustor. Additionally the lobed injector provides higher fluctuation than the flat injector.
- In the combustion test, both injectors show two different combustion modes and their transition; weak and strong combustion.
- The ignition for both injectors is precipitated by the pseudo-shock wave in vicinity of the exit of the combustor.
- The mode transition is supposed to accompany a detonation wave.
- The enhancement of the lobed injector in the mixing performance is not observed in the combustion test because the combustion in the present study is not a mixing-controlled reaction. The pseudo-shock wave and the detonation waves change the mixing and combustion performance significantly.

References

[1] Chun, J., Scheuermann, T., von Wolfersdorf, J., and Weigand, B., "Experimental Study on Combustion Mode Transition in a Scramjet with Parallel Injection," *14th AIAA/AHI Space Planes and Hypersonic Systems and Technologies Conference*, 2006, AIAA 2006-8063.

[2] Strickland, J. H., Selerland, T., and Karagozian, A. R., "Numerical simulations of a lobed fuel injector," *Physcis of Fluids*, Vol. 10, 1998, pp. 2950–2964.

[3] Gerlinger, P., Kasal, P., Stoll, P., and Brueggemann, D., "Experimental and Theoretical Investigation on

2D and 3D Parallel Hydrogen/Air Mixing in a Supersonic Flow," *International Symposium on Airbreathing Engines*, 2001, ISABE 2001-1019.

[4] Smith, L., Majamaki, A., Lam, I., Delabroy, O., Karagozian, A., and Marble, F., "Mixing Enhancement in a lobed injector," *Physics of Fluids*, Vol. 9, No. 3, March 1997, pp. 667–678.

[5] Majamaki, A., Smith, O., and Karagozian, A., "Passive Mixing Control via Lobed Injectors in High-Speed Flow," *AIAA Journal*, Vol. 41, No. 4, April 2003, pp. 623–632.

[6] Willert, C. and Jarius, M., "Planar flow field measurements in atmospheric and pressurized combustion chambers," *Experiments in Fluids*, Vol. 33, 2002, pp. 931–939.

[7] Heiser, W. H. and Pratt, D. T., *Hypersonic Airbreathing Propulsion*, AIAA, 1994.

[8] Matsuo, K., Miyazato, Y., and Kim, H.-D., "Shock train and Pseudo-shock phenomena in internal gas flow," *Progress in Aerospace Sciences*, Vol. 35, 1999, pp. 33–100.

[9] Papamoschou, D. and Roshko, A., "The compressible turbulent shear layer : an experimental study," *Journal of Fluid Mechanics*, Vol. 197, 1988, pp. 453–477.

[10] Gerlinger, P. and Brüggemann, D., "Numerical Investigation of Hydrogen Strut Injections into Supersonic Airflows," *Journal of Propulsion and Power*, Vol. 16, No. 1, January 2000, pp. 22–28.

[11] Scheuermann, T., Chun, J., and von Wolfersdorf, J., "Experimental Investigations of Scramjet Combustor Characteristics," *15th AIAA International Space Planes and Hypersonic Systems and Technologies Conference*, 2008, AIAA 2008-2552.

[12] Rogers, R. C. and Jr., C. J. S., "Chemical Kinetics Analysis of Hydrogen-Air Ignition and Reaction Times," Tech. rep., NASA, 1981, NASA TP-1856.

[13] Sunami, T., Kodera, M., and Nakahashi, K., "Considerations on Mixing and Combustion of a Scramjet Engine - Transition Processes from Weak to Intensive Combustion Mode," *Journal of the Japan Society for Aeronautical and Space Sciences*, Vol. 50, 2002, pp. 22–29.